

See discussions, stats, and author profiles for this publication at: <https://www.researchgate.net/publication/26238334>

Drying of the Silica/PVA Suspension: Effect of Suspension Microstructure

ARTICLE *in* LANGMUIR · JULY 2009

Impact Factor: 4.46 · DOI: 10.1021/la804112b · Source: PubMed

CITATIONS

22

READS

82

4 AUTHORS, INCLUDING:



Sunhyung Kim

LG Chem

12 PUBLICATIONS 59 CITATIONS

SEE PROFILE



Kyung Hyun Ahn

Seoul National University

112 PUBLICATIONS 1,831 CITATIONS

SEE PROFILE

Drying of the Silica/PVA Suspension: Effect of Suspension Microstructure

Sunhyung Kim, Jun Hee Sung, Kyung Hyun Ahn,* and Seung Jong Lee

School of Chemical and Biological Engineering, Seoul National University, San 56-1 Shillim-dong, Gwanak-gu, Seoul 151-744, Korea

Received December 14, 2008. Revised Manuscript Received March 3, 2009

The particle/polymer/solvent suspension system shows complicated microstructure. When the suspension system experiences an industrial process such as coating and drying, the system experiences microstructural change. In this study, we investigated the microstructural change during the drying of a silica/polyvinyl alcohol (PVA) suspension, with an emphasis on suspension stability. We controlled the amount of PVA adsorption on the silica surface by adjusting the pH (1.5, 3.6, and 9) of the silica/PVA suspension. The amount of adsorption was measured to increase with decreasing pH, and the degree of flocculation in the silica/PVA suspension became stronger with decreasing pH. However, through the measurement of stress development during drying and the observation of film microstructure after drying, we found that the more strongly flocculated suspension became a more disperse, close-packed film after drying. By evaluating the potential energy, we could suggest the role of adsorbed polymers in structural change during the drying of the silica/PVA suspension. As pH decreases, the adsorbed polymers could bridge the particles and lead to a flocculated suspension before drying. As the solvent evaporates during drying, the adsorbed polymers introduce steric repulsion between approaching particles, leading to a change from flocculated to dispersed microstructure. This implies that the required silica/PVA film performance and the microstructure of the silica/PVA suspension can be tailored through controlling the polymer adsorption in suspension.

Introduction

Coating and printing technology is important in manufacturing electronic devices such as displays,¹ capacitors,² solar cells,^{3,4} and so on. Industrial coating materials such as ink, slurry, and paste form complicated microstructures because they contain various components such as particles, binders, additives, and solvents. Thus, in this field, one often encounters problems involving dispersion instability such as flocculation, sedimentation, and coagulation. Because they have long been industrial challenges, many theoretical and practical efforts have been carried out to overcome these problems by controlling electrostatic^{5–7} and steric repulsions.^{8–12}

Because most coating products are used in the solid state, understanding their drying behavior is as important as understanding their flow behavior in the liquid state. The stress development due to frustrated shrinkage during drying leads to severe coating defects such as cracking, curling, delamination, and deformation. Hence, understanding the origin of stress development as well as controlling the stress distribution is

important to achieving defect-free coating products. Stress development during drying can be measured by the beam deflection method,^{13–18} which is related to in-plane stress in a coating layer adhered to a rigid substrate.¹⁹ The measurement of the stress development based on the beam deflection method was employed in various kinds of coating research, including the origin of stress development in a polymer solution^{13,20} and suspension,^{21,22} the effect of solvent formulation on the drying of a polymer solution,²³ the effect of binder on the drying of a suspension,^{24–26} and the relation between suspension stability and drying behavior.^{21,22,27} However, there exist only a few studies that relate the suspension microstructure caused by the addition of polymer to drying, even though the use of a polymer in a suspension has a vast number of applications in industry.

In this study, we investigate the relation between the microstructure of suspension and drying behavior of silica/PVA suspensions. We characterize the microstructure of silica/PVA suspensions at different pH values by measuring the zeta potential, particle size, turbidity, and PVA adsorption on silica surface. The drying behavior of the suspensions prepared at various pH values are characterized in terms of the stress development and film microstructure. Results are discussed in terms of potential

*Corresponding author. E-mail: ahnnet@snu.ac.kr. Tel: +82-2-880-8322.

- (1) Su, P. J.; Sha, Y. A.; Shiu, J. W. *J. Soc. Inf. Display* **2008**, *16*, 441–449.
- (2) Taho, Y.; Ronald, V. O. *J. Eng. Design* **2004**, *15*, 447–457.
- (3) Shah, V. G.; Wallace, D. B. *Proceedings of the IMAPS 37th Symposium on Microelectronics*, Long Beach, CA, 2004.
- (4) Doshi, P.; Mejjia, J.; Tate, K.; Rohatgi, A. *IEEE Trans. Electron Devices* **1997**, *44*, 1417–1424.
- (5) Sun, J.; Velamakanni, B. V.; Gerberich, W. W.; Francis, L. F. *J. Colloid Interface Sci.* **2004**, *280*, 387–399.
- (6) Sun, J.; Gerberich, W. W.; Francis, L. F. *Prog. Org. Coat.* **2007**, *59*, 115–121.
- (7) Brown, R. F. G.; Carr, C.; Taylor, M. E. *Prog. Org. Coat.* **1997**, *30*, 195–206.
- (8) Chang, S. H.; Gupta, R. K.; Ryan, M. E. *J. Rheol.* **1992**, *36*, 273–287.
- (9) de Laat, A. W. M.; Derks, W. P. T. *Colloid Surf., A* **1993**, *71*, 147–153.
- (10) Heath, D.; Tadros, T. F. *J. Colloid Interface Sci.* **1983**, *93*, 320–328.
- (11) Otsubo, Y. *J. Colloid Interface Sci.* **1986**, *112*, 380–386.
- (12) Sakellariou, P.; Strivens, T. A.; Petit, F. *Colloid Polym. Sci.* **1995**, *273*, 279–287.
- (13) Croll, S. G. *J. Coat. Technol.* **1978**, *50*, 33–38.
- (14) Perera, D. Y.; Eynde, D. V. *J. Coat. Technol.* **1981**, *53*, 39–44.
- (15) Payne, J. A.; McCormick, A. V.; Francis, L. F. *Rev. Sci. Instrum.* **1997**, *68*, 4564–4568.

- (16) Martinez, C. J.; Lewis, J. A. *Langmuir* **2002**, *18*, 4689–4698.
- (17) Petersen, C.; Heldmann, C.; Johannsmann, D. *Langmuir* **1999**, *15*, 7745–7751.
- (18) Tirumkudulu, M. S.; Russel, W. B. *Langmuir* **2004**, *20*, 2947–2961.
- (19) Corcoran, E. M. *J. Paint. Technol.* **1969**, *41*, 635–640.
- (20) Croll, S. G. *J. Appl. Polym. Sci.* **1979**, *23*, 847–858.
- (21) Chiu, R. C.; Garino, T. J.; Cima, M. J. *J. Am. Ceram. Soc.* **1993**, *76*, 2257–2264.
- (22) Chiu, R. C.; Cima, M. J. *J. Am. Ceram. Soc.* **1993**, *76*, 2769–2777.
- (23) Vaessen, D. M.; McCormick, A. V.; Francis, L. F. *Polymer* **2002**, *43*, 2267–2277.
- (24) Lewis, J. A.; Blackman, K. A.; Ogden, A. L.; Payne, J. A.; Francis, L. F. *J. Am. Ceram. Soc.* **1996**, *79*, 3225–3234.
- (25) Wedin, P.; Lewis, J. A.; Bergstr. L. *J. Colloid Interface Sci.* **2005**, *290*, 134–144.
- (26) Wedin, P.; Martinez, C. J.; Lewis, J. A.; Daicic, J.; Bergstr. L. *J. Colloid Interface Sci.* **2004**, *272*, 1–9.
- (27) Guo, J. J.; Lewis, J. A. *J. Am. Ceram. Soc.* **1999**, *82*, 2345–2358.

energy, which accounts for the effect of both adsorbed and nonadsorbed polymers on the microstructure of the suspension and its drying behavior.

Experimental Method

Materials. We prepared suspensions composed of silica, poly (vinyl alcohol) (PVA), and water. Silica particles were supplied by Aldrich (Ludox HS-30) in the form of a 30 wt % electrically stabilized aqueous silica suspension with an average particle size of 12 nm, a specific surface area of 220 m²/g, and a density of 2.37×10^3 kg/m³, according to the supplier. PVA having a molecular weight of $(31-50) \times 10^3$ g/mol, a degree of hydrolysis of 87 to 88%, and a density of 1.27×10^3 kg/m³ was supplied by Aldrich. A 10 wt % PVA solution was dissolved in deionized water at 353 K for 3 h as a stock solution. The weight fraction of silica/PVA/DI water was determined to be 10:5:85. The pH of silica/PVA suspensions was adjusted by adding 1 M HCl solution. Because the time dependence was observed from a preliminary experiment, the experiments were always carried out with the samples stirred for 24 h at room temperature.

Characterization of Silica/PVA Suspension. The silica/PVA suspension was characterized by measuring the amount of adsorption, turbidity, zeta potential, and particle size. The amount of PVA adsorption on the silica surface was measured by the solution depletion method²⁸ using a total organic carbon analyzer (Apollo 9000, Teledyne Instruments, CA), which can measure the carbon concentration in the liquid. The carbon concentration was measured by burning the known amount of liquid. The suspension was diluted to 400 ppm silica and 200 ppm PVA to meet the detectable range of the TOC analyzer, which is from 10 to 500 ppm of PVA in the liquid. It was centrifuged for 1 h at 10 000 rpm²⁹ to separate the PVA solution from the suspension. The concentration of PVA that remained in the supernatant after centrifugation was measured and compared to the original concentration. The reduced concentration of PVA was regarded as equivalent to the adsorbed amount of PVA on the silica surface. A turbidity measurement was performed using the optical analyzer³⁰ (Turbiscan Laboratory, Formulation, France) that is based on the multiple light scattering principle. Twenty milliliters of a silica/PVA suspension contained in a glass bottle whose length is 60 mm was placed in the apparatus. A pulsed near-infrared light source ($\lambda = 850$ nm) illuminates the sample at 25 mm from the bottom, and synchronous transmitted and backscattered fluxes were measured. Turbidity was estimated from the transmittance under the assumption that the incident flux is not absorbed by the sample. Turbidity ranges from 0%, which is equivalent to that of water, to 100% for a sample that is optically opaque. Turbidity was measured three times and averaged. The zeta potential and particle size were measured using dynamic light scattering (Zetasizer nano zs, Malvern Instruments Ltd., U.K.). Silica/PVA suspensions were diluted to 1/100–3/1000 of the initial concentration prior to measurement to meet the detectable range of the apparatus. Silica suspension was not detected since it satisfied the detectable range of apparatus. Both the zeta potential and particle size were measured three times and averaged.

Characterization of Drying Behavior. The drying behavior of a suspension was characterized by measuring the stress development and weight loss during drying. Stress development of a coating layer was characterized in situ during drying using the cantilever deflection method that is schematically displayed in Figure 1a. The technique¹⁵ measures the deflection of the free end of the cantilever with the other end held between rigid stainless steel clamps. The cantilever is a silicon wafer with a

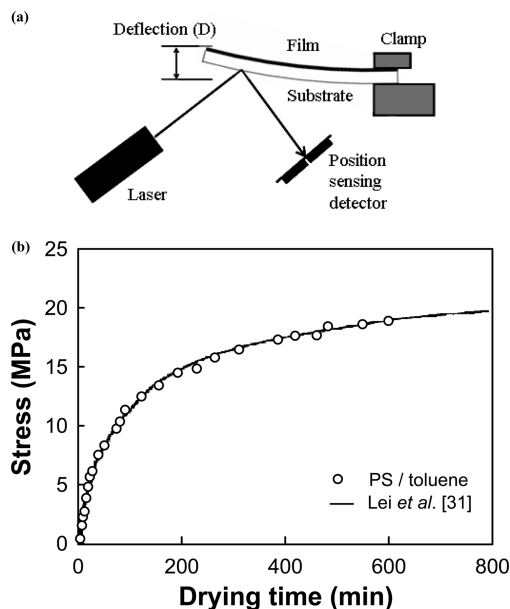


Figure 1. (a) Schematic diagram of the stress measurement apparatus and (b) the comparison of the stress development result of 15 wt % polystyrene/toluene (○) measured with the apparatus in our group and that of Lei et al.³¹

thickness of 530 μ m and dimensions of 70 mm \times 6 mm. A thin gold layer is sputtered under the cantilever to enhance reflectivity. Deflection of the cantilever during drying is measured as follows: a 1 mW diode laser generated from the light source (LM-6501NAP, Lanics Co, Korea) is reflected under the cantilever and reaches the position-sensitive photodiode (PSDM4, Thorlabs) that transforms the beam position to an electric signal with voltage. The position evolution during drying is recorded with a data acquisition system. A calibration was conducted prior to every experiment in order to relate the deflection of the cantilever and the electric signal captured by the position-sensitive photodiode. Upon calibration, the cantilever was taken out and positioned under the doctor's blade. Then the suspension was applied to the cantilever over an area of 45 mm \times 6 mm. The blade gap was adjusted to ensure that the final dried film thickness is 11 ± 1 μ m. The coated cantilever was positioned next to the drying chamber, which controls the environment to a relative humidity of $10 \pm 1\%$ and a drying temperature of 300 ± 2 K.

The deflection data were transformed to the biaxial in-plane stress σ using the following formula¹⁹

$$\sigma = \frac{dE_s t_s^3}{3t_c l^2 (t_s + t_c)(1 - \nu_s)} + \frac{dE_c (t_s + t_c)}{l^2 (1 - \nu_c)} \quad (1)$$

where d , E , t , l , and ν are the deflection, elastic modulus, thickness, and Poisson ratio, respectively. Subscripts s and c designate the substrate and coating film after drying, respectively. The measured stress by the cantilever deflection in the equilibrium state is always smaller than the true stress, and the second term of eq 1 compensates for the stress relief in a coating by the bending of the cantilever. However, this second term can be ignored if the modulus of the film is much smaller than that of the substrate. Other assumptions introduced by Corcoran were employed in this experiment: spherical deflection within the limited elastic region of the coating and substrate, isotropic mechanical properties, and good adhesion.¹⁹ The stress measurement with a 15 wt % polystyrene in toluene solution was conducted and compared with the previous result.³¹ Figure 1b

(28) Paik, U.; Hackley, V. A.; Lee, H.-W. *J. Am. Ceram. Soc.* **1999**, *82*, 833–840.

(29) Rachas, I.; Tadros, T. F.; Taylor, P. *Colloids Surf., A* **2000**, *161*, 307–319.

(30) Mengual, O.; Meunier, G.; Cayre, I.; Puech, K.; Snabre, P. *Colloids Surf., A* **1999**, *152*, 111–123.

(31) Lei, H.; Payne, J. A.; McCormick, A. V.; Francis, L. F.; Gerberich, W. W.; Scriven, L. E. *J. Appl. Polym. Sci.* **2001**, *81*, 1000–1013.

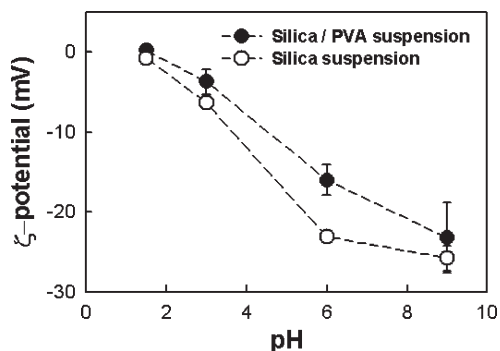


Figure 2. Zeta potential of a silica/PVA suspension (●) and a silica suspension (○).

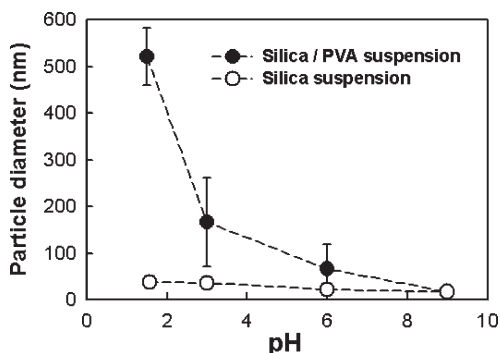


Figure 3. Number-averaged particle size of the silica/PVA suspension (●) and the silica suspension (○)

shows good agreement with the previous result, which confirms the validity of our apparatus.

Weight loss during drying was separately measured in the drying chamber under the drying condition equivalent to the stress measurement experiment. An analytical balance (GR-200, A&D Company, Japan) whose resolution is 0.1 mg was mounted on the drying chamber. A small stage suspended under the bottom of the balance is located in the drying chamber. The cantilever coated with a silica/PVA suspension by a doctor's blade was brought onto the stage in the drying chamber, and the weight loss was monitored by a data acquisition system. After the drying experiment, the surface microstructure of the dried film was observed using a scanning electron microscope (JSM-840A, JEOL, Japan).

Results

Characterization of Silica/PVA at Various pH Values.

The microstructure of a silica/PVA suspension was characterized at different pH values (1.5, 3, 6, and 9) in terms of the zeta potential, particle size, and turbidity. To understand the effect of PVA on the suspension microstructure, a 10 wt % pure silica suspension was prepared as well. The zeta potential of both the silica/PVA suspension and the silica suspension was measured, with the lowest at pH 9 (−23 and −25 mV, respectively) and the value increasing with decreasing pH, as shown in Figure 2. In particular, the isoelectric point, which is the point of zero charge, was around pH 2, which well coincides with previous studies.^{32–34} The zeta potential of silica particles in a silica/PVA suspension was slightly less negative than that of the

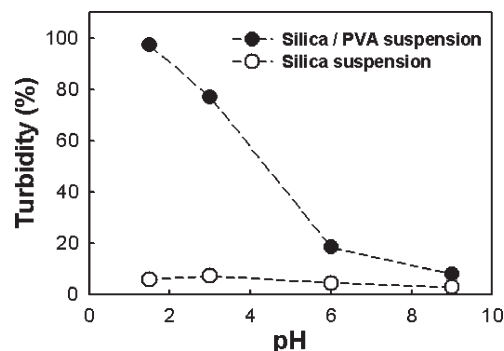


Figure 4. Turbidity measurement of the silica/PVA suspension (●) and the silica suspension (○).

silica suspension over the whole pH range that we have covered. This result can be attributed to the screening effect of nonionic polymer on the electrically charged particle edge, which results in the decrease in negative charges on the silica surface.³⁵

The particle size measured with both the silica/PVA suspension and the silica suspension at various pH values is displayed in Figure 3. The silica suspension without PVA did not show any significant particle size dependence on pH. The particle size was measured to be 16.8 ± 0.7 nm at pH 9, which is somewhat larger than that from the information supplied by the manufacturer, 12–14 nm. Considering that the deviation may result from the hydrodynamic radius measured by dynamic light scattering, the particles in a silica suspension at pH 9 seems to remain as primary particles. As the pH decreases to 1.5, the particle size increases to 37.5 ± 0.63 nm, which means that three or four primary particles form one flocculated particle. On the contrary, the measured particle size in the silica/PVA suspension was 17.7 ± 1.3 nm at pH 9. However, it increased upon decreasing the pH to 520.6 ± 61.6 nm at pH 1.5, which means that the particles are severely flocculated. The turbidity measurement displayed in Figure 4 supports the result of the particle size measurement.

For the silica suspension without PVA, the turbidity was measured to be 2.8 and 5% at pH 9 and 1.5, respectively. Meanwhile, the measured turbidity of silica/PVA suspensions was 7.9% at pH 9 and significantly increased to 97.3% at pH 1.5, which means that the silica/PVA suspension at pH 1.5 is as much as optically opaque. The particle size and turbidity increasing with decreasing pH only for the silica/PVA suspension means that PVA plays a key role in microstructural rearrangement as the pH changes. The role of PVA in the microstructural change of the silica/PVA suspension can be explained by PVA adsorption as a function of pH. Figure 5 shows the amount of PVA adsorption on the silica surface, which indicates that the amount of adsorption is smallest at pH 9 and increases as the pH decreases.

The increase in PVA adsorption with decreasing pH is due to a gradual increase in the affinity of silica surface with PVA. Tadros³⁶ showed the same tendency—increasing adsorption with decreasing pH—and suggested that the main mechanism of PVA adsorption on the silica surface is the hydrogen bonding between the hydroxyl group (−OH) in PVA and the silanol group (−SiOH) on the silica surface. As the pH decreases, the number of silanol groups on the silica surface increases, and the degree of PVA adsorption increases more under acidic conditions than under basic conditions. Later, Tadros et al.³³ showed the progressive increase in flocculation with decreasing pH, followed by the maximum flocculation at the isoelectric point,

(32) Chu, W.-B.; Yang, J.-W.; Liu, T.-J.; Tiu, C.; Guo, J. *Colloids Surf., A* **2007**, *302*, 1–10.

(33) Tadros, T. F. *J. Colloid Interface Sci.* **1978**, *64*, 36–47.

(34) So, J.-H.; Oh, M.-H.; Lee, J.-D.; Yang, S.-M. *J. Chem. Eng. Jpn.* **2001**, *34*, 262–268.

(35) Ece, I.; Alemdar, A.; Gungor, N.; Hayashi, S. *J. Appl. Polym. Sci.* **2002**, *86*, 341–346.

(36) Tadros, T. F. *J. Colloid Interface Sci.* **1974**, *46*, 528–540.

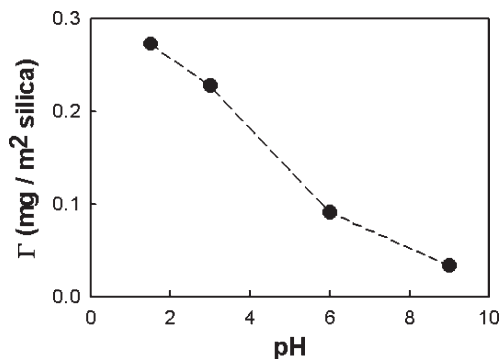


Figure 5. Amount of PVA adsorbed on the silica surface (Γ) in the silica/PVA suspension from pH 1.5 to 9.

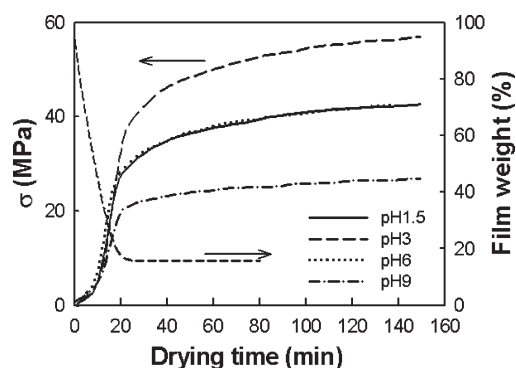


Figure 6. Stress development during drying (σ) of silica/PVA suspensions

and suggested that the adsorption behavior with varying pH affects the microstructure and properties of the suspension via either flocculation through bridging or stabilization through steric repulsion. In the silica/PVA suspension, more flocks are likely to form because the number of silanol groups on the silica surface increases with lowered pH and the hydroxyl groups in PVA can be adsorbed more easily on the silanol groups of the silica particles. This flocculation should be distinguished from the agglomeration or coagulation of bare particles that are not surrounded by polymers. As a result, the suspension experiences microstructural change due to the increasing amount of PVA adsorption as the pH decreases.

Characterization of Drying Behavior. In general, the binder-free suspension exhibits a sharp maximum stress peak, followed by an abrupt relaxation to almost zero stress level as demonstrated by Chiu et al.²² However, when the binder is present in the suspension, it has a significant influence on stress development. Lewis et al.²⁴ found that the stress history of the alumina/PVB suspension exhibited a trend similar to that for the PVB solution. The stress history of the alumina/PVB suspension and PVB solution did not exhibit a stress decrease after the maximum stress. However, the stress history of the alumina/PVB/plasticizer suspension and the PVB/plasticizer solution showed a stress decrease after the maximum stress. Wedin et al.^{25,26} also studied the effect of a polymer binder on the stress history of a CaCO₃ suspension. They showed two-stage stress development—an initial stress peak due to capillary pressure followed by a second larger stress increase due to the solidification of the polymer-rich phase. Figure 6 shows the stress (σ) development and the weight loss measurement during the drying of the silica/PVA suspension at various pH values. Film weight loss shows that solvent

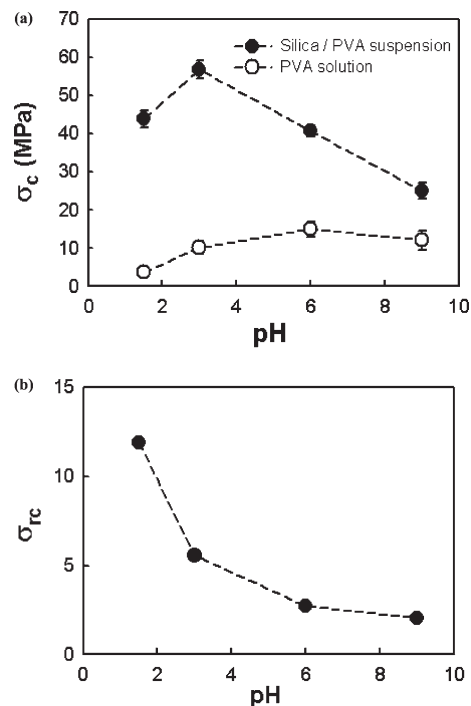


Figure 7. (a) Characteristic stress (σ_c) of the silica/PVA suspension (●) and the PVA solution (○) and (b) the relative characteristic stress (σ_{rc})

evaporation ended at around 20 min and did not show any considerable dependence on pH within the measurable range of the balance.

All of the stress development curves during the drying of silica/PVA suspensions with various pH values appear to approach their asymptotic maximum stress without a stress decrease afterward. However, each curve shows a different asymptotic stress depending on the pH. For example, the stress development during the drying of the suspension at pH 9 exhibits a steep increase of up to 20 min and approaches an asymptotic stress, 25 MPa at 150 min of drying time. However, the suspension at pH 3 shows a stress rise over 20 min and reaches 60 MPa at 150 min of drying time, but it still increases even after 150 min. The effect of pH on stress development can be attributed to the combination of two causes that affect stress development. First, the microstructure of the silica/PVA suspension that is already affected by pH influences the stress development. Second, the property of PVA itself in the PVA/silica suspension is influenced by pH and affects stress development. To understand the effect of suspension microstructure on stress development precisely, the two causes need to be distinguished, and the contribution of PVA should be excluded in analyzing the stress development. Therefore, the stress development of PVA solution at the same pH with the silica/PVA suspension was measured. The stress history of the PVA solution exhibited a stress rise to an asymptote without decrease. The characteristic stress (σ_c) was defined as the stress development at 150 min of drying time, and σ_c of the silica/PVA suspension and PVA solution are compared in Figure 7a. σ_c of the silica/PVA suspension is higher than σ_c of the PVA solution at each pH because of the addition of inorganic particles.³⁷ σ_c of the PVA solution depends on the pH—it is highest at pH 6 and lowest at pH 1.5. Even though there is no definite evidence to explain the

(37) Perera, D. Y. *Prog. Org. Coat.* **2004**, *50*, 247–262.

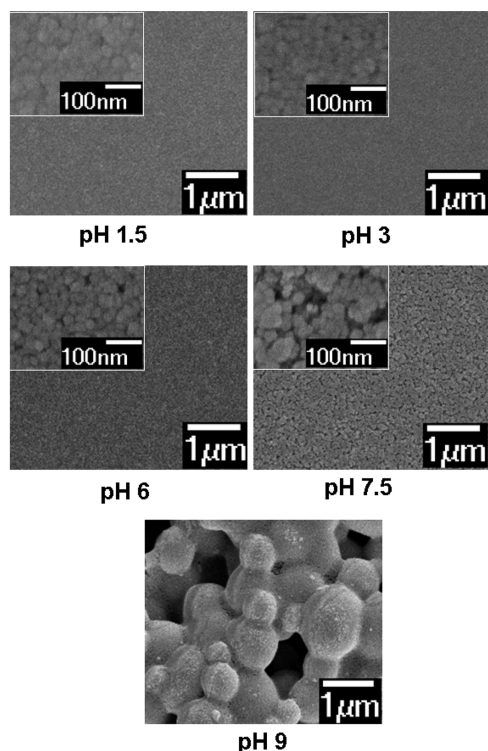


Figure 8. SEM images of a dried film surface prepared from the silica/PVA suspension with varied pH.

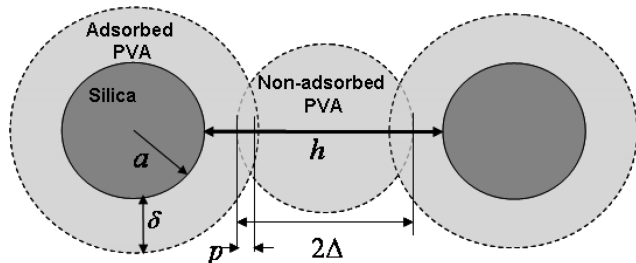


Figure 9. Schematics of interaction between two particles when PVA is adsorbed.

reason for the stress decrease at pH 1.5, a similar tendency is observed and attributed to the decomposition of PVA.^{38–40} Alexy et al.³⁹ found that the thermal stability of PVA severely deteriorates when it is prepared from the strong acidic solution. Thus, the lowest σ_c of PVA solution at pH 1.5 may be attributed to the deterioration of PVA itself under the strong acidic condition, thus the decomposition of PVA results in a decrease of the σ_c of the silica/PVA suspension at pH 1.5. To exclude the effect of PVA decomposition on the stress development of the silica/PVA suspension, we defined the relative characteristic stress (σ_{rc}) which divides σ_c of the silica/PVA suspension by σ_c of the PVA solution. The results are displayed in Figure 7b.

σ_{rc} is the lowest at pH 9 and increases as the pH decreases, resulting in the highest value at pH 1.5. This trend is in accordance with the increasing amount of PVA adsorption with decreasing pH as in Figure 5. This means that a large amount of PVA adsorption results in a high σ_{rc} after drying. To gain a

Table 1. Amount of PVA Adsorbed and Corresponding Parameter Values for the Calculation of Potential Energy

pH	1.5	3	6	9
adsorption (mg/m ²)	0.273	0.227	0.091	0.034
adsorbed PVA (vol%)	0.57	0.47	0.19	0.07
nonadsorbed PVA (vol%)	4.18	4.28	4.56	4.68
adsorbed layer thickness (nm)	5.64	4.7	1.88	0.71
Φ_{s0}	0.29	0.24	0.11	0.04
D_{Sc} (nm)	5.6	4.7	1.9	0.7

better understanding of the effect of PVA adsorption on the relative maximum stress, the film microstructure after drying has been compared in Figure 8 because the drying stress is closely related to the drying microstructure.

SEM images of a dried film surface obtained in the order of flocculation from the least flocculated (pH 9) to the most flocculated (pH 1.5) silica/PVA suspension are displayed in Figure 8. As the flocculation increases with a larger amount of adsorption in the liquid state, the dried film has a denser, more packed microstructure from pH 9 to 1.5. Finally, the dried film obtained from the strongly flocculated suspension at pH 1.5 has a close-packed, dense microstructure. In particular, the film obtained from the least flocculated suspension at pH 9 displays a very unique microstructure, with significantly large pores. A related study of the film microstructure prepared from the suspension at pH 9 will be reported later.

From the relation among the amount of PVA adsorption in the silica/PVA suspension, stress development during drying, and film microstructure after drying, it is clear that the σ_{rc} increases, forming more dense microstructure as pH decreases as follows: the lowest σ_{rc} is obtained from the most sparse film microstructure at pH 9 caused by the least amount of PVA adsorption, and the highest σ_{rc} at pH 1.5 arises from the most consolidated microstructure by a large amount of PVA adsorption. From the relation between the suspension microstructure and film microstructure, the least flocculated suspension becomes the most porous dried microstructure whereas the most flocculated suspension becomes the most dense dried microstructure. This trend is opposite to the result of the previous study^{21,27} in which a more flocculated suspension resulted in more porous and heterogeneous dried microstructure while a less flocculated suspension resulted in denser, dried microstructure. The main difference is the origin of flocculation. The flocculation of the silica/PVA suspension in this work is subjected to PVA adsorption, whereas the flocculation of the binder-free suspension in their work is subjected to the electrostatic potential, which is not directly related to the binder. Therefore, PVA adsorption in the silica/PVA suspension has a significant influence on the final film property that results in the opposite trend in the film property compared to that obtained from the binder-free suspension. The effect of PVA adsorption on dried film microstructure and stress will be discussed in terms of potential energy in the next section.

Discussion

The PVA in the silica/PVA suspension exists in two different states, adsorbed and nonadsorbed PVA. Adsorbed polymer chains induce not only steric repulsion but also bridging attraction in addition to affecting the electrostatic and van der Waals interaction, and nonadsorbed polymers induce a depletion attraction. To understand the effect of PVA adsorption on structure change during drying, the effect of polymer adsorption was evaluated in terms of the potential energy. The schematic diagram

(38) Finch, C. A., *Polyvinyl Alcohol: Developments*, 2nd ed.; Wiley: New York, 1992; Chapter 1.

(39) Alexy, P.; Káčová, D.; Kríak, M.; Bakos, D.; Simková, B. *Polym. Degrad. Stab.* **2002**, *78*, 413–421.

(40) Vijayalakshmi, S. P.; Madras, G. *J. Appl. Polym. Sci.* **2006**, *100*, 4888–4892.

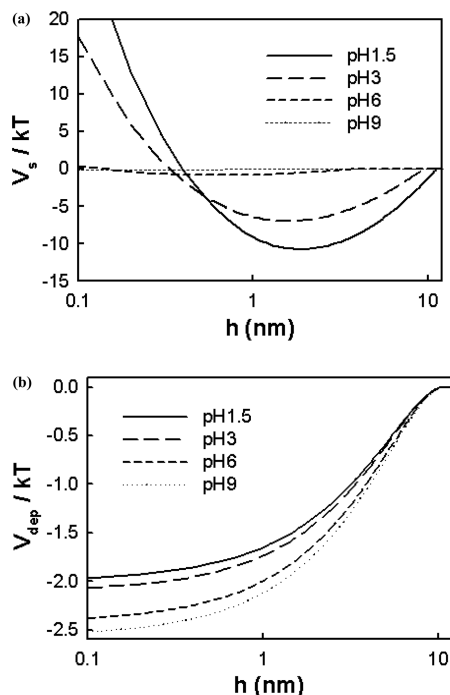


Figure 10. (a) Interaction energy due to adsorbed polymer layers (V_s) including both steric repulsion and bridging attraction and (b) interaction energy by the depletion attraction (V_{dep}) of the silica/PVA suspension at various pH values

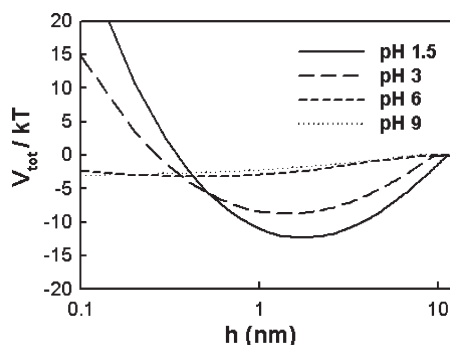


Figure 11. Total potential energy (V_{tot}) with particle separation (h) for the silica/PVA suspension at various pH values.

of two particles with adsorbed polymer for the calculation of the potential energy was displayed in Figure 9.

In Figure 9, a , δ , h , and p are the radius of a silica particle, the adsorption layer thickness, the closest distance of the surface between two approaching particles, and the interpenetration distance, respectively. Δ , which was calculated to 5.43 nm⁴¹ for the silica/PVA suspension, refers to the range of the depletion effect that is proportional to the radius of gyration of the polymer. Because the range over which the particle–particle interaction occurs changed depending on the thickness of adsorbed layer, the adsorption layer thickness was calculated from the measured amount of PVA adsorbed on silica and the surface area of silica, with the following assumptions: the volume profile of PVA in the adsorption layer is constant, regardless of the distance from the silica surface,⁴¹ and the volume concentration of PVA in the adsorption layer is the same as that of bulk PVA. The calculated thickness of the adsorption layer including the

total volume fraction of adsorbed PVA and nonadsorbed PVA is summarized in Table 1.

The modified equation for spherical particles⁴² based on the scaling theory of polymer adsorption^{43,44} has been employed to compute the interaction energy due to adsorbed polymer layers. The interaction energy (V_s) including both steric repulsion and the bridging attraction is expressed by

$$V_s = \pi r \left(\frac{\alpha_{sc} k_B T}{a_m^3} \right) \Phi_{s0}^{9/4} D_{sc} \left\{ - \frac{16 \Gamma D_{sc}}{\Gamma_0} \ln \left(\frac{2\delta}{h} \right) + \frac{4 D_{sc}^{5/4}}{2^{5/4}} \left(\frac{8 \Gamma}{\Gamma_0} \right)^{9/4} \left[\frac{1}{h^{1/4}} - \frac{1}{(2\delta)^{1/4}} \right] \right\} \quad (2)$$

where r is the radius of a particle with adsorbed polymer layer, a_m is the segment length of a monomer defined as the mesh size of the Flory–Huggins lattice, and α_{sc} is a numerical constant that is related to osmotic pressure. In this calculation, the values of α_{sc} and a_m were used in the form of $\alpha_{sc} k_B T / a_m^3 = 3 \times 10^5 \text{ N/m}^2$ on the basis of the previous study.⁴⁵ Φ_{s0} is the polymer concentration at the saturated surface, and D_{sc} is the effective thickness of the adsorbed polymer.⁴³ Both Φ_{s0} and D_{sc} can be obtained from the volume profile of the adsorbed polymer, which can be measured by neutron scattering.⁴⁶ The value of Φ_{s0} was adjusted by considering both the experimental result for the volume profile of PVA that is adsorbed on the polystyrene latex⁴⁶ and the fact that it increases with decreasing pH because the adsorption site increases with decreasing pH. The value of D_{sc} was set equal to δ . Γ/Γ_0 is the coverage where Γ is the total amount of polymer adsorbed on a single surface and Γ_0 is the adsorbed amount at saturation. The parameters are correlated by $\Gamma_0 = 4 D_{sc} \Phi_{s0} / a_m^3$.⁴⁵ The coverage Γ/Γ_0 was adjusted to 0.35 and assumed to be constant independent of pH because both the amount of adsorption and the number of adsorption sites increase as the pH decreases. The first term within the brace in eq 2 represents the attraction whereas the second term accounts for excluded volume repulsion. Suspension stability that is influenced by either bridging attraction or steric repulsion was determined by the relative magnitude of these two contributions. Specific values of parameters used for the calculation are summarized in Table 1. Figure 10a shows V_s for the silica/PVA suspension at various pH values. Every curve has a similar tendency. Attraction occurs at $h = 2\delta$ ($h = 11.2 \text{ nm}$ at pH 1.5) and becomes stronger as the particles approach. As the particles come closer at about $h = \delta/15$ ($h = 0.4 \text{ nm}$ at pH 1.5), the repulsion develops as a result of the compression of adsorbed polymers. The range and magnitude of repulsion increase with decreasing pH as a result of an increased number of adsorbed polymers. It is noteworthy that the depth of bridging attraction is very sensitive to Γ/Γ_0 . For example, at $\Gamma/\Gamma_0 = 0.5$, the potential well formed by the bridging attraction disappears. Because it is hard to know the exact value of Γ/Γ_0 at each pH, the magnitude of the bridging attraction is somewhat unclear. However, the steric repulsion always increases as the pH decreases, independent of the coverage Γ/Γ_0 .

(42) Runkana, V.; Somasundaran, P.; Kapur, P. C. *Chem. Eng. Sci.* **2006**, *61*, 182–191.

(43) De Gennes, P. G. *Macromolecules* **1981**, *14*, 1637–1644.

(44) De Gennes, P. G. *Macromolecules* **1982**, *15*, 492–500.

(45) Klein, J.; Rossi, G. *Macromolecules* **1998**, *31*, 1979–1988.

(46) Cosgrove, T.; Crowley, T. L.; Ryan, K.; Webster, J. R. P. *Colloids Surf.* **1990**, *51*, 255–269.

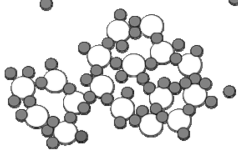
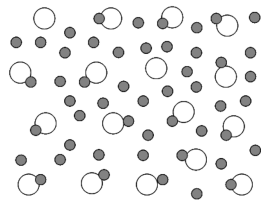
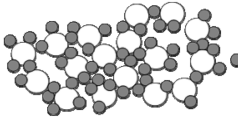
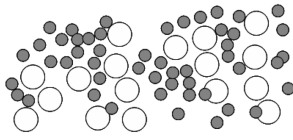
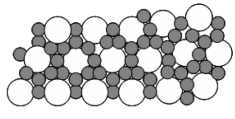
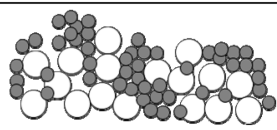
pH	3	9
Before drying	 Flocculated	 Dispersed
During drying	 Strong steric repulsion by large amount of adsorbed polymers	 Weak steric repulsion by small amount of adsorbed polymers
After drying	 Dispersed drying microstructure	 Flocculated drying microstructure

Figure 12. Suggested schematic mechanism of microstructure change during drying as a function of the pH of the silica/PVA suspension.

The depletion interaction (V_{dep}) was calculated as follows.⁴¹

$$V_{\text{dep}} = -2\pi a P_2 \left(\Delta + \delta - p - \frac{h}{2} \right)^2 \quad \text{for } \delta > p \quad (3)$$

$$V_{\text{dep}} = -2\pi a P_2 \left(\Delta - \frac{h}{2} \right)^2 \quad \text{for } \delta < p \quad (4)$$

P_2 is the osmotic pressure of the bulk polymer solution. The penetration distance p refers to the maximum thickness of interpenetration between the adsorption layer and nonadsorbed polymer. It was calculated to be 4.8 nm, and it is larger than δ of the suspension above pH 3. Thus, eq 3 was used for the suspension at pH 1.5 whereas eq 4 was used for the suspension at pH 3, 6, and 9. Figure 10b illustrates V_{dep} that was derived from eqs 3 and 4. V_{dep} becomes weak as the pH decreases because the volume fraction of nonadsorbed PVA decreases with increasing pH. In particular, depletion attraction changes depending on the bulk polymer concentration, and it will be described more in conjunction with solvent evaporation in the discussion of total potential energy.

Figure 11 shows the total potential energy (V_{tot}), which is expressed by $V_{\text{tot}} = V_s + V_{\text{dep}} + V_{\text{vdw}} + V_e$ as a function of h at different pH values of the silica/PVA suspension. The van der Waals attraction (V_{vdw})⁴⁷ and the electrostatic repulsion (V_e)⁴⁸ were calculated to decrease with decreasing pH as a result of the increasing adsorption layer and the decreasing zeta potential, respectively. As the pH decreases from pH 9 to 1.5, the suspensions show stronger repulsion at very short distances (e.g., shorter than about $\delta/15$), which is introduced by larger amounts of adsorbed polymer.

From the potential energy evaluation and experimental observations, the microstructural change in the silica/PVA suspen-

sion during drying can be explained as follows. As the pH increases to 9, the suspension becomes less flocculated as the electrostatic repulsion is enhanced, as evidenced by the zeta potential. As the solvent evaporates, the particles flocculate and the polymer segregates because the depletion attraction increases, leading to inhomogeneous, porous microstructure. In addition, polymer bridging that was rare in the suspension state due to high electrostatic repulsion becomes more significant as it dries, which prevents the particles from rearrangement. On the contrary, as pH decreases to pH 1.5, the flocculated structure is formed because of the reduced electrostatic repulsion and the bridging effect. As drying proceeds, the adsorbed polymers induce steric repulsion and suppress depletion flocculation, leading to close-packed film microstructure. We propose the mechanism of microstructural change during drying at different pH values (e.g., pH 3 and 9) with the schematic diagram in Figure 12.

Conclusions

The microstructural change in the silica/PVA suspension during the drying process was investigated. As the pH increases to pH 9, the suspension becomes less flocculated, and the particles flocculate and the polymer segregates as the solvent evaporates, leading to inhomogeneous and porous microstructure. On the contrary, as the pH decreases to 1.5, the flocculated structure is formed. As drying proceeds, the particles become less flocculated, leading to close-packed film microstructure. From the fact that the required film performance and the microstructure of the silica/PVA suspension can be tailored through controlling the polymer adsorption in suspension, the present work will provide a useful pragmatic understanding of coating and printing applications when they deal with particle/polymer suspension systems.

Acknowledgment. This study was supported by a grant from the cooperative R&D Program funded by the Korea Research Council of Industrial Science and Technology, Republic of Korea.

(47) Vold, M. J. *J. Colloid Sci.* **1961**, *16*, 1–12.

(48) Rawson, S.; Ryan, K.; Vincent, B. *Colloids Surf.* **1988**, *34*, 89–93.